
FUSION OF MOVEMENT AND NAÏVE PREDICTIONS FOR POINT FORECASTING IN UNIVARIATE RANDOM WALKS

Cheng Zhang[†]

School of Electrical and Electronics Engineering
Hubei Polytechnic University
Huangshi, China
zcheng582dx@gmail.com

v4

ABSTRACT

Point forecasting in univariate random walks is an important but challenging research topic that has attracted numerous researchers. Unfortunately, traditional regression methods for this task often fail to surpass naïve benchmarks due to data unpredictability. From a decision fusion perspective, this study proposes a novel forecasting method, which is derived from a variant definition of random walks, where the random error term for the future value is expressed as a positive random error multiplied by a direction sign. This method, based on the fusion of movement and naïve predictions, does not require a loss function for optimization and can be optimized by estimating movement prediction accuracy on the validation set. This characteristic prevents the fusion method from reverting to traditional regression methods and allows it to integrate various machine learning and deep learning models for movement prediction. The method's efficacy is demonstrated through simulations and real-world data experiments. It reliably outperforms naïve forecasts with moderate movement prediction accuracies, such as 0.55, and is superior to baseline models such as the ARIMA, linear regression, MLP, and LSTM networks in forecasting the S&P 500 index and Bitcoin prices. This method is particularly advantageous when accurate point predictions are challenging but accurate movement predictions are attainable, translating movement predictions into point forecasts in random walk contexts.

Keywords Random walk · Fusion · Movement prediction · Naïve prediction · Point forecasting

1 Introduction

A random walk is a type of time series in which each data point is a random increment from the previous point, characterized by a memoryless property and stepwise random changes [Pearson \(1905\)](#). A wide range of real-world phenomena can be modeled as random walks, from financial time series, such as stock prices and exchange rates, to physical phenomena, such as Brownian motion. The dependence from one time step to the next in a random walk series provides a certain degree of consistency, avoiding the large jumps seen in a purely random series [Wergen et al. \(2012\)](#). Therefore, strong autocorrelation can be observed between two adjacent data points in a random walk, and the whole series is often nonstationary, with the mean and/or variance changing over time.

Another key characteristic of a random walk is that future values are considered unpredictable based on past values alone, as predicting a random walk is akin to predicting a series of random events [Fama \(1995\)](#); [Zhang \(1999\)](#). Despite significant efforts, including complex modeling using both machine learning and deep learning algorithms, along with various levels of data fusion for data augmentation [Thakkar and Chaudhari \(2021\)](#), forecasting models often struggle to effectively recognize meaningful patterns in random walk series and typically underperform naïve forecasting, which assumes that the future value of the series will be the same as the most recent value [Ellwanger and Snudden \(2023\)](#); [Hewamalage et al. \(2023\)](#). Recent studies have proposed various time-frequency decomposition methods that have

[†]: <https://orcid.org/0000-0002-4150-3371>

been shown to outperform naïve forecasts in random walk forecasting [Hewamalage et al. \(2023\)](#); [Zhang et al. \(2023\)](#). However, these methods often include future information in the training data, leading to data leakage and a higher forecasting accuracy [Hewamalage et al. \(2023\)](#); [Wu et al. \(2022\)](#); [Zhang et al. \(2015\)](#). When data leakage is explicitly avoided during data preprocessing, the prediction accuracy often falls below that of the naïve forecast [Hewamalage et al. \(2023\)](#). This superiority of naïve forecasts underscores the significant challenge of point forecasting in random walks [Moosa and Burns \(2014\)](#).

Prediction tasks in different areas often involve constructing mathematical models that attempt to describe real phenomena and using these models to forecast future outcomes [Frigg and Hartmann \(2018\)](#). However, most regression methods implemented for random walk forecasting presuppose a mapping from historical values to future values, which does not align with the concept of random walks, where the future value depends solely on the current value with a random increment and higher-order autocorrelations rapidly diminish toward zero. This misalignment in the underlying prediction mechanisms can significantly contribute to the suboptimal performance of these methods, particularly when the assumed patterns and dependencies do not exist in the data with the true random walk nature.

This study addresses the challenge of random walk point forecasting from a novel perspective, focusing on translating movement predictions into point forecasts, the potential of which remains less investigated. By introducing a sign representing the movement direction of the future value, the random error term in the definition of random walks, which is independent and identically distributed (i.i.d.), can be expressed as a positive i.i.d. random error multiplied by this sign. With regard to prediction, the sign can be estimated via movement prediction, and the estimation of the positive error for the future point can be obtained empirically based on both the estimation of movement prediction accuracy and the residual of the naïve forecast on the historical data. Therefore, from this variant definition of random walks, the one-step-ahead point forecasting of a univariate random walk can theoretically be derived from the fusion of movement and naïve predictions. More importantly, this fusion method does not require a loss function for optimization. Instead, it can be optimized by estimating movement prediction accuracy on the validation set, avoiding reverting to traditional regression methods, which often face bottlenecks in random walk forecasting. Furthermore, movement prediction can be achieved using various machine learning and deep learning algorithms, which are advancing rapidly.

To prove the effectiveness of the proposed fusion method in random walk point forecasting, this study first conducted a theoretical analysis to compare the fusion result with the naïve forecast using the mean squared error (MSE). Then, both simulations and real-data experiments were conducted to empirically validate the performance of the proposed method. The simulations employed a simulated random walk series to examine the impact of different levels of movement prediction accuracies on fusion outcomes. The real-world forecasting experiments were based on two univariate time series—Standard and Poor’s 500 (S&P 500) index and Bitcoin (BTC) price series—owing to their data availability and typical characterization as random walks. Movement predictions for the real-data forecasting tasks were achieved using a nu-support vector machine (nu-SVM) with a set of technical indicators as the model inputs. Additionally, the proposed method was compared with various baseline models, including the autoregressive integrated moving average (ARIMA), linear regression, multilayer perceptron (MLP), and long short-term memory (LSTM) networks, to validate its effectiveness.

This study makes three significant contributions to the literature:

- By leveraging binary classification, which is typically considered unrelated to regression tasks, point forecasting of random walks that surpass naïve forecasts becomes possible. In financial time series forecasting, complex feature engineering using external information can enhance movement and point predictions. However, point predictions generally remain less accurate than naïve forecasts, and predicting the direction of movement (a binary classification task) is often easier than forecasting the exact value of a target variable [Taylor \(2008\)](#). The proposed method shows that random walk point forecasting can be predicted to a certain degree by incorporating movement prediction with a certain accuracy.
- This study highlights directions for future improvements in random walk forecasting. Rather than developing end-to-end regression models, we could instead focus on enhancing movement prediction accuracy. The findings of this study show that accurate binary classification is equivalent to accurate regression in univariate random walk forecasting.
- The fusion process can be considered a classification-to-regression conversion. Given a set of diverse predictions with both binary and continuous data types, the proposed method offers an approach for converting binary data into continuous data, making it possible to combine predictions with diverse data types for better decision making.

Overall, this study offers a novel perspective for point forecasting in univariate random walks, demonstrating its effectiveness and paving the way for improved forecasting accuracy.

The remainder of this paper is organized as follows. Section 2 provides background information on random walk forecasting. Section 3 presents the details of the proposed fusion method, including a theoretical analysis of the fusion results. Section 4 provides the experimental results of the proposed and baseline models. Section 5 discusses the concerns and limitations of the study. Finally, Section 6 concludes the study and discusses future research directions.

2 Background

Since a large number of studies on random walk forecasting focus on the financial sector and univariate random walk series across various fields often exhibit similar characteristics, the background information in this section is predominantly derived from studies on financial time series forecasting.

2.1 Point forecasting of random walks

Accurate point forecasting for random walks has always been challenging. In financial markets, the behavior of financial instruments often resembles a random walk, presenting few, if any, discernible patterns for analysts to exploit [Fama \(1995\)](#). Nonetheless, several forecasting methods have been developed to address this challenge.

Fundamental analysis, once a mainstay in financial forecasting, has waned in popularity because of its inefficiency and heavy reliance on a forecaster’s ability to interpret the data [Deboeck \(1994\)](#); [Rouf et al. \(2021\)](#). Conversely, statistical methods such as ARIMA and generalized autoregressive conditional heteroskedasticity (GARCH) models provide a structured mathematical approach for time series analysis. However, these methods often fail to capture the nonlinear patterns and complex interdependencies that characterize real-world financial data [Adhikari and Agrawal \(2014\)](#); [Cheng et al. \(2015\)](#).

With the advent of machine learning, techniques such as artificial neural networks (ANNs) and support vector regression (SVR) have demonstrated their ability to identify hidden patterns in historical data. However, these methods depend heavily on feature engineering and face challenges related to model complexity, particularly when handling large datasets [Jiang \(2021\)](#). These limitations underscore the ongoing need for more effective forecasting methods that can handle the intricacies of financial data.

Deep learning has emerged as a transformative force in this context. LSTM networks, a specialized form of recurrent neural networks (RNNs), have achieved significant success by capturing temporal dependencies in data sequences [Hochreiter and Schmidhuber \(1997\)](#). These capabilities have positioned LSTM networks as preferred forecasting models over traditional statistical and machine learning methods for tasks such as price forecasting in financial markets [Durairaj and Mohan \(2019\)](#); [Lara-Benítez et al. \(2021\)](#); [Nosratabadi et al. \(2020\)](#); [Sezer et al. \(2020\)](#).

Furthermore, convolutional recurrent neural networks (CRNNs), which integrate the spatial pattern recognition capabilities of convolutional neural networks (CNNs) with the temporal analysis strengths of RNNs, have been effectively applied to price forecasting, illustrating the potential for discerning spatiotemporal patterns in complex time series data [Shi et al. \(2017\)](#); [Tsantekidis et al. \(2020\)](#). Moreover, transformer-based models, such as Vision Transformer (ViT) and Autoformer, have been adapted to process financial time series due to their ability to capture intricate patterns and dependencies over extended periods [Malibari et al. \(2021\)](#); [Wu et al. \(2021\)](#). ViT, originally designed for image classification, utilizes self-attention mechanisms to manage global interactions within sequential data, making it adaptable for financial time series analysis. Autoformer, designed specifically for time series forecasting, incorporates decomposition blocks and autocorrelation mechanisms to enhance its effectiveness in modeling long-term temporal dependencies. These properties make transformer-based approaches increasingly useful for understanding and predicting the dynamics of time series.

In general, deep learning models offer significant advantages by automatically learning and adapting to complex patterns, including both linear and nonlinear dependencies, with minimal reliance on domain-specific knowledge [Bengio \(2011\)](#); [Goodfellow et al. \(2016\)](#). However, the effectiveness of these advanced predictive models in forecasting random walk series remains debated. While deep learning models are celebrated for their sophisticated pattern recognition capabilities, they are often criticized for not consistently outperforming simpler models, such as naïve forecasts, in practice [Ellwanger and Snudden \(2023\)](#); [Hewamalage et al. \(2023\)](#). The ongoing debate underscores the complexity and challenges involved in developing models that can reliably forecast random walks.

2.2 Movement prediction of random walks

Movement prediction and point forecasting often share the same input characteristics, with differences in the interpretation of the output. Point forecasting can be converted to binary classification by comparing the forecasted point

to the previous value or using activation functions, such as the sigmoid function, to squash the regression result to a probability of the future point moving upward or downward.

Various machine learning and deep learning models that utilize a range of advanced techniques have been proposed for movement prediction. Classical and machine learning models employ technical indicators, price data, and fundamental data for movement prediction [Raza \(2017\)](#); [Sezer et al. \(2017\)](#), whereas neural networks integrated with selective trading strategies have been shown to be effective in movement prediction [Das et al. \(2018\)](#); [Yang et al. \(2017\)](#). Additionally, LSTM and gated recurrent unit (GRU) networks, incorporating technical indicators such as moving average convergence divergence (MACD), demonstrate their utility in handling movement estimation for stock markets [Nelson et al. \(2017\)](#); [Troiano et al. \(2018\)](#).

CNN-based methods, which were originally designed for image recognition, can be applied to classify 2D images transformed from financial time series data. These models can also incorporate advanced techniques, such as the Gramian Angular Field (GAF), moving average mapping (MAM), and Candlestick with converted image data, proving to be particularly effective in environments with complex data representations [Chen et al. \(2016\)](#); [Gudelek et al. \(2017\)](#); [Sezer and Ozbayoglu \(2018\)](#).

Text mining techniques also contribute significantly to movement prediction. Combining more information, such as by leveraging sentiment analysis from social media and word embeddings from financial news, can generally improve model performance [Matsubara et al. \(2018\)](#); [Wang et al. \(2018\)](#); [Yoshihara et al. \(2014\)](#). Depending on the complexity of the markets and data availability, the movement prediction accuracy in financial time series typically falls between 0.55 and 0.80 [Bustos and Pomares-Quimbaya \(2020\)](#).

Notably, point forecasting and movement prediction were explored independently. The potential of translating accurate binary classification to superior point forecasting has been insufficiently studied.

3 Method

This section discusses the details of the proposed fusion method, by which movement predictions and naïve forecasts are integrated for point forecasting. Derived from a variant definition of random walks, the fusion method was introduced, followed by a theoretical analysis of the fusion results, which emphasizes how improvements in movement prediction accuracy can influence fusion outcomes. Aligned with the aim of this study, which is to demonstrate the effectiveness of the proposed fusion method for random walk point forecasting, this section omits details on movement prediction models and only discusses the fusion process at the decision level. Any model capable of producing meaningful movement predictions can be integrated to improve point forecasts through the proposed fusion method.

3.1 Fusion of movement and naïve predictions

Given a random walk series y , the value of the data point at time step t depends only on the value of the data point at the previous time step $t - 1$ and the random increment ϵ_t , which is i.i.d. and is typically assumed to follow a normal distribution with mean 0 and variance σ^2 [De Gooijer \(2017\)](#). This relationship is defined as follows:

$$y_t = y_{t-1} + \epsilon_t, \tag{1}$$

where y_{t-1} is the point value at time step $t - 1$ and is known as the naïve forecast of y_t , and $\epsilon_t \sim \mathcal{N}(0, \sigma^2)$. We can further introduce a sign to determine the direction of the increment between two adjacent points and refine the representation of ϵ_t as a positive i.i.d. random error term multiplied by this sign. Through this modification, the random walk can be formulated as:

$$y_t = y_{t-1} + M_t \cdot \epsilon_t^+; \epsilon_t^+ > 0, \tag{2}$$

where $M_t \in \{-1, 1\}$ is a sign factor that indicates the changing direction of the point value at time step t compared with the point value at time step $t - 1$ and ϵ_t^+ is a positive i.i.d. random error term that represents the magnitude of

the increment between these two adjacent points. As these positive increments are uncorrelated, they are theoretically unpredictable. Nonetheless, ϵ_t^+ can further be expressed as a multiplication of two positive values:

$$y_t = y_{t-1} + M_t \cdot c_t \cdot \bar{\epsilon}; c_t > 0, \bar{\epsilon} > 0, \quad (3)$$

where $\bar{\epsilon}$ is the mean of the absolute residuals of the naïve forecast calculated from the historical data, which is a constant positive value. The term c_t , which is positive and i.i.d., is introduced as a weight that controls the magnitude of the increment at time step t . Suppose a simplified scenario in which the increment between two adjacent points is constant for future time steps; then, c_t can be set to a fixed value in advance. Consequently, the forecast of future value, \hat{y}_t , can be expressed as follows:

$$\hat{y}_t = y_{t-1} + \hat{M}_t \cdot c \cdot \bar{\epsilon}; c > 0, \bar{\epsilon} > 0, \quad (4)$$

where \hat{M}_t is the movement prediction, c is a fixed scalar, and $c \in R$. The point forecast, based on (4), can be regarded as a fusion of movement and naïve predictions. Given that y_{t-1} and $\bar{\epsilon}$ are determined from the historical data and \hat{M}_t is provided by movement prediction, optimizing the fusion result is equivalent to finding the optimal value of c . Suppose movement prediction \hat{M}_t is provided by a binary classification model, and the value of c is given; then, the fusion result for the whole test set can be calculated using Algorithm 1.

Algorithm 1 Fusion of movement and naïve predictions for point forecasting in random walks

Inputs:

Y : Array of historical values

\hat{M} : Array of movement predictions for the test set

α : Proportion of the dataset allocated to the test set

c : Fixed weight attached to the mean absolute residual of the naïve forecast

Output:

P : Array of fusion results for the test set

1. Compute the split index (k) and segment the data:

$k \leftarrow \lfloor \text{length}(Y) \times (1 - \alpha) \rfloor$

$Y_{\text{train}} \leftarrow Y[1 : k]$

$Y_{\text{test}} \leftarrow Y[k + 1 : \text{end}]$

2. Generate naïve forecasts for the Y_{train} :

$Y_{\text{naïve}} \leftarrow Y_{\text{train}}[1 : \text{end} - 1]$

3. Determine the residuals from naïve forecasts:

$R \leftarrow Y_{\text{train}}[2 : \text{end}] - Y_{\text{naïve}}$

4. Calculate the mean of the absolute residuals:

$\bar{\epsilon} \leftarrow \text{mean}(\text{abs}(R))$

5. Initialize the prediction array and set the initial forecast:

$P \leftarrow []$

$Y_{\text{last}} \leftarrow Y_{\text{train}}[\text{end}]$

6. Each point in Y_{test} is forecasted by integrating the movement predictions:

for $i \leftarrow 1$ to $\text{length}(Y_{\text{test}})$ **do**

$\Delta \leftarrow c \cdot \bar{\epsilon} \times M[i]$ // Increment calculation using the mean absolute residual and direction

$Y_{\text{forecast}} \leftarrow Y_{\text{last}} + \Delta$

$P.\text{append}(Y_{\text{forecast}})$

$Y_{\text{last}} \leftarrow Y_{\text{test}}[i]$

end for

7. Return P

3.2 Theoretical analysis of the fusion results

This subsection presents a theoretical analysis of the performance of the fusion method by comparing the MSE, the fundamental metric for quantifying the accuracy of point forecasting, between the fusion and naïve predictions on the test set. This theoretical analysis also provides a method to determine the optimal value of c to achieve the best fusion result. Assuming that both the training and test sets are sufficiently large, with respective counts of M and N data points, and that the movement prediction results in $n_{correct}$ correct directions and $n_{incorrect}$ incorrect directions for the test set, the MSE of the fusion results on the test set can be expressed as follows:

$$\begin{aligned}
 MSE^{\text{fusion}} &= \frac{1}{N} \left(\sum_{t \in \text{testset}} (y_t - \hat{y}_t)^2 \right) \\
 &= \frac{1}{N} \left(\sum_{t \in \text{correct}} (y_t - \hat{y}_t^{\text{correct}})^2 + \sum_{t \in \text{incorrect}} (y_t - \hat{y}_t^{\text{incorrect}})^2 \right) \\
 &= \frac{1}{N} \left(\sum_{t \in \text{correct}} \left[(y_{t-1} + M_t \cdot \epsilon_t^+) - (y_{t-1} + \hat{M}_t \cdot c \cdot \bar{\epsilon}) \right]^2 \right. \\
 &\quad \left. + \sum_{t \in \text{incorrect}} \left[(y_{t-1} + M_t \cdot \epsilon_t^+) - (y_{t-1} + \hat{M}_t \cdot c \cdot \bar{\epsilon}) \right]^2 \right) \\
 &= \frac{1}{N} \left(\sum_{t \in \text{correct}} (\epsilon_t^+ - c \cdot \bar{\epsilon})^2 + \sum_{t \in \text{incorrect}} (\epsilon_t^+ + c \cdot \bar{\epsilon})^2 \right) \\
 &= \frac{1}{N} \left(\sum_{t \in \text{correct}} ((\epsilon_t^+)^2 - 2c \cdot \epsilon_t^+ \bar{\epsilon} + c^2 \cdot \bar{\epsilon}^2) + \sum_{t \in \text{incorrect}} ((\epsilon_t^+)^2 + 2c \cdot \epsilon_t^+ \bar{\epsilon} + c^2 \cdot \bar{\epsilon}^2) \right)
 \end{aligned} \tag{5}$$

Correspondingly, the MSE of the naïve forecast on the test set is:

$$\begin{aligned}
 MSE^{\text{naïve}} &= \frac{1}{N} \left(\sum_{t \in \text{testset}} (y_t - y_{t-1})^2 \right) \\
 &= \frac{1}{N} \left(\sum_{t \in \text{testset}} (y_{t-1} + M_t \cdot \epsilon_t^+ - y_{t-1})^2 \right) \\
 &= \frac{1}{N} \left(\sum_{t \in \text{correct}} (\epsilon_t^+)^2 + \sum_{t \in \text{incorrect}} (\epsilon_t^+)^2 \right)
 \end{aligned} \tag{6}$$

For $MSE^{\text{fusion}} < MSE^{\text{naïve}}$, the following inequality should be fulfilled:

$$\begin{aligned}
 \sum_{t \in \text{correct}} ((\epsilon_t^+)^2 - 2c \cdot \epsilon_t^+ \bar{\epsilon} + c^2 \cdot \bar{\epsilon}^2) + \sum_{t \in \text{incorrect}} ((\epsilon_t^+)^2 + 2c \cdot \epsilon_t^+ \bar{\epsilon} + c^2 \cdot \bar{\epsilon}^2) &< \sum_{t \in \text{correct}} (\epsilon_t^+)^2 + \sum_{t \in \text{incorrect}} (\epsilon_t^+)^2 \\
 \sum_{t \in \text{correct}} (c^2 \cdot \bar{\epsilon}^2 - 2c \cdot \epsilon_t^+ \bar{\epsilon}) + \sum_{t \in \text{incorrect}} (2c \cdot \epsilon_t^+ \bar{\epsilon} + c^2 \cdot \bar{\epsilon}^2) &< 0 \tag{7} \\
 n_{\text{correct}} \cdot c^2 \cdot \bar{\epsilon}^2 - 2c \cdot \bar{\epsilon} \cdot \sum_{t \in \text{correct}} \epsilon_t^+ + n_{\text{incorrect}} \cdot c^2 \cdot \bar{\epsilon}^2 + 2c \cdot \bar{\epsilon} \cdot \sum_{t \in \text{incorrect}} \epsilon_t^+ &< 0
 \end{aligned}$$

Based on the law of large numbers (LLN) and that ϵ_t^+ is a positive i.i.d. random error, when both $n_{correct}$ and $n_{incorrect}$ are sufficiently large $\sum_{t \in correct} \epsilon_t^+$ approximates $n_{correct} \cdot \bar{\epsilon}$ and $\sum_{t \in incorrect} \epsilon_t^+$ approximates $n_{incorrect} \cdot \bar{\epsilon}$. Therefore, (7) can be expressed as follows:

$$\frac{n_{correct} \cdot c^2 \cdot \bar{\epsilon}^2 - 2c \cdot \bar{\epsilon} \cdot (n_{correct} \cdot \bar{\epsilon}) + n_{incorrect} \cdot c^2 \cdot \bar{\epsilon}^2 + 2c \cdot \bar{\epsilon} \cdot (n_{incorrect} \cdot \bar{\epsilon})}{(2c + c^2) \cdot n_{incorrect}} < 0 < \frac{(2c - c^2) \cdot n_{correct}}{(2c + c^2) \cdot n_{incorrect}} \quad (8)$$

Given that c is a positive scalar, the threshold of $ACC^{movement}$ for $MSE^{fusion} < MSE^{naive}$ on the test set is:

$$ACC^{movement} = \frac{n_{correct}}{n_{incorrect} + n_{correct}} > \frac{2 + c}{4} \quad (9)$$

Therefore, if $ACC^{movement}$ is less than 0.5, the fusion prediction will always be inferior to the naïve forecast, regardless of the value of c . In addition, we can obtain the MSE difference between the naïve and fusion results for the test set based on (5) and (6) and simplify the result according to the LLN and that both c and $\bar{\epsilon}$ are positive and constant values:

$$\begin{aligned} MSE^{naive} - MSE^{fusion} &= \frac{1}{N} \left(\sum_{t \in correct} (\epsilon_t^+)^2 + \sum_{t \in incorrect} (\epsilon_t^+)^2 \right) \\ &\quad - \frac{1}{N} \left(\sum_{t \in correct} ((\epsilon_t^+)^2 - 2c \cdot \epsilon_t^+ \bar{\epsilon} + c^2 \cdot \bar{\epsilon}^2) \right) \\ &\quad + \sum_{t \in incorrect} ((\epsilon_t^+)^2 + 2c \cdot \epsilon_t^+ \bar{\epsilon} + c^2 \cdot \bar{\epsilon}^2) \\ &= \frac{1}{N} \left(\sum_{t \in correct} (2c \cdot \epsilon_t^+ \bar{\epsilon} - c^2 \cdot \bar{\epsilon}^2) \right) \\ &\quad - \sum_{t \in incorrect} (2c \cdot \epsilon_t^+ \bar{\epsilon} + c^2 \cdot \bar{\epsilon}^2) \\ &\approx \frac{1}{N} (2c \cdot \bar{\epsilon} \cdot (n_{correct} \cdot \bar{\epsilon}) - n_{correct} \cdot c^2 \cdot \bar{\epsilon}^2 \\ &\quad - 2c \cdot \bar{\epsilon} \cdot (n_{incorrect} \cdot \bar{\epsilon}) - n_{incorrect} \cdot c^2 \cdot \bar{\epsilon}^2) \\ &= \frac{1}{N} (n_{correct} \cdot (2c - c^2) \bar{\epsilon}^2 - (2c + c^2) n_{incorrect} \cdot \bar{\epsilon}^2) \\ &= (4c \cdot ACC^{movement} - c^2 - 2c) \cdot \bar{\epsilon}^2 \end{aligned} \quad (10)$$

According to (10), the difference between the MSEs of the naïve and fusion forecasts on the test set depends on the $ACC^{movement}$, the fixed scalar c , and the constant value $\bar{\epsilon}$. Notably, (10) can be regarded as a quadratic function of c , which attains its maximum value when

$$c = 2 \cdot ACC^{movement} - 1 \quad (11)$$

Based on the above analysis, interestingly, the optimal value of c depends only on $ACC^{movement}$. Given that when $ACC^{movement} \in (0.5, 1)$, the movement prediction is meaningful, we can obtain the corresponding optimal value

of c , which falls within the range between 0 and 1. If we set a large value for c , the threshold of ACC^{movement} for improvement from the naïve forecast must also be high. Based on (11), when the ACC^{movement} is only 0.51, setting a small value for c , such as 0.01, can theoretically ensure that the fusion forecast outperforms the naïve forecast in terms of the MSE. When the ACC^{movement} is equal to 1, the optimal value of c is 1. Under these conditions, we can achieve the maximum potential improvement from the fusion process, which is given by the value of $\bar{\epsilon}^2$. This improvement represents the full potential of the fusion method. The value assigned to the weight c for the fusion prediction represents a trade-off between the likelihood of outperforming the naïve forecast and the magnitude of the improvement. When c is fixed, an increase in ACC^{movement} directly increases the discrepancy in the MSE between the naïve and fusion forecasts. In a real forecasting scenario where ACC^{movement} is unknown, we can use the movement prediction accuracy on the training set or validation set as an estimation of ACC^{movement} and set c based on (11). Because the RMSE is the root of the MSE, obtaining the requirement for $RMSE^{\text{fusion}} < RMSE^{\text{naive}}$ is equivalent to obtaining that for $MSE^{\text{fusion}} < MSE^{\text{naive}}$.

According to (4), (10), and (11), point forecasting based on the fusion method will be affected only by ACC^{movement} , and the fusion result is optimized by setting the value of c based on an estimation of ACC^{movement} . This finding implies that accurate movement prediction can be translated to accurate point forecasting in univariate random walks.

4 Experimental results

To evaluate the effectiveness of the proposed method for random walk forecasting, this study employed a two-pronged experimental approach, providing a holistic view of its performance across different conditions. Initially, the method was tested using simulated data to understand its performance under different levels of ACC^{movement} . Subsequently, the method was applied to real-world data to assess its practical utility and effectiveness in actual forecasting scenarios.

The experiments were conducted on a cloud-based Jupyter notebook service, which provided adaptable virtual machines with CPUs for simulated experiments and L4 GPUs for training baseline models such as MLP and LSTM. The software environment included Python 3.8 with core libraries such as TensorFlow 2.3 and NumPy 1.19. All the methods in the experiments were evaluated using the MSE and MAE. The formulas for these metrics are as follows:

$$MSE = \frac{1}{N} \sum_{i=1}^N (y_i - \hat{y}_i)^2, \quad (12)$$

$$MAE = \frac{1}{N} \sum_{i=1}^N |y_i - \hat{y}_i| \quad (13)$$

where N denotes the test set size, \hat{y}_i denotes the predicted value, and y_i denotes the actual value.

4.1 Experiment 1: Simulated data

Figure 1 shows a simulated random walk series of 2,500 steps generated for evaluating the proposed fusion method. Each step of the random walk was drawn from a normal distribution with a mean of zero and a standard deviation of one, reflecting typical stochastic fluctuations. The cumulative sum of these steps constitutes a random walk path. To maintain all the values within a positive range, an initial positive offset of 50 units was applied to the entire series. The last 200 data points were selected as the test set, while the remaining data points were used to calculate the value of $\bar{\epsilon}$.

To specifically analyze the impact of ACC^{movement} on the performance of the fusion method, the simulated experiments presuppose the existence of movement predictions at different accuracy levels. By controlling the accuracy of the movement predictions, we can assess how the fusion method performs relative to a naïve forecasting approach under varying conditions. Correspondingly, the weight c was set based on (11) to optimize the fusion outcome for each trial. This adjustment demonstrated the full potential of the proposed method.

To evaluate the significance of the differences observed between the fusion forecasts and the naïve forecasts, the fusion process was repeated 100 times at each accuracy level, with all trials using random movement predictions of the same accuracy. Therefore, 100 independent MSE and MAE measures were generated at each ACC^{movement} level, as shown in Figure 2. Each box plot represents a set of 100 independent MSE or MAE measures at a certain ACC^{movement} level. Although variation was observed among each set, the fusion result generally improved as ACC^{movement} increased, and except when $ACC^{\text{movement}} = 0.5$, the fusion forecasts generally achieved lower MSEs and MAEs than did the

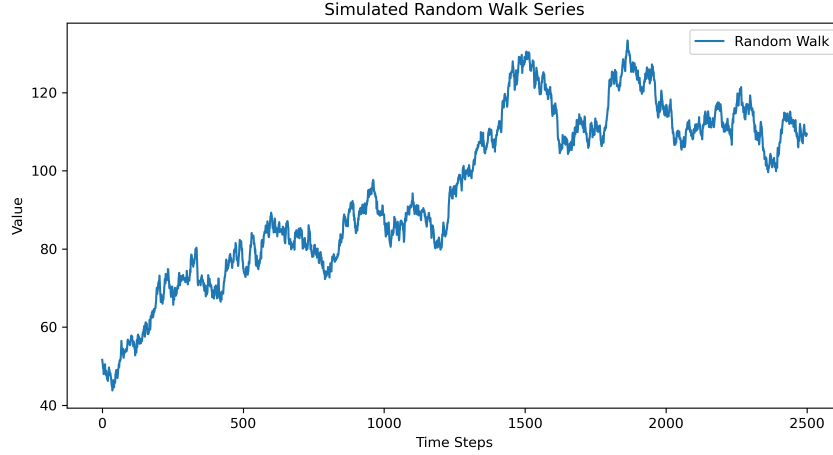


Figure 1: The simulated random walk series.

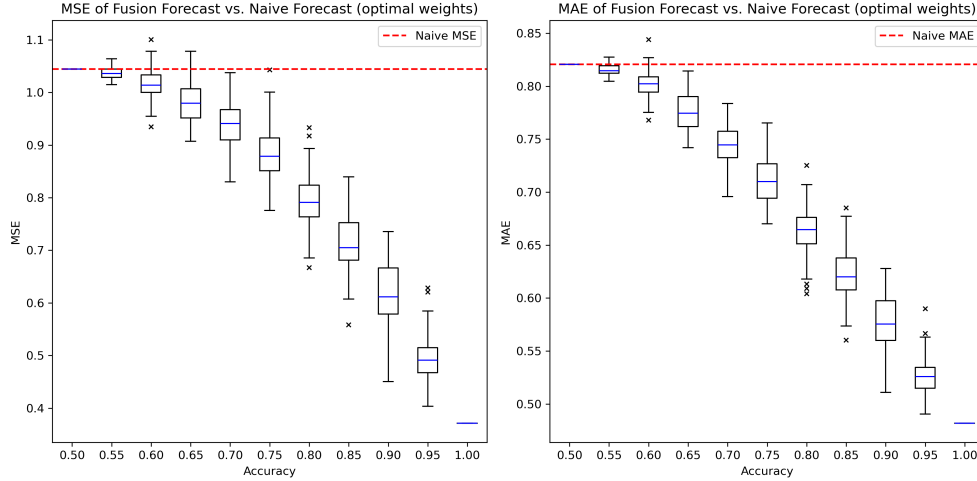


Figure 2: Fusion forecasts across different movement prediction accuracies.

naïve forecasts. When the movement accuracy is equal to 0.5, the movement prediction is essentially equivalent to a random guess. Under these conditions, the proposed fusion method does not offer any improvement over the naïve prediction. Consequently, the optimal prediction in this scenario is simply the naïve prediction itself. Subsequently, the one-sample Wilcoxon signed-rank test was conducted to determine whether, at each accuracy level, the median values of the differences between the MSEs or MAEs of the fusion forecasts and those of the naïve forecasts significantly deviated from zero. The MSEs and MAEs of the naïve and fusion forecasts and the results of the Wilcoxon tests are summarized in Table 1. Notably, the two p values derived when $ACC^{\text{movement}} = 0.55$ are equal to zero, indicating a statistically significant enhancement of the fusion forecast over the naïve forecast, confirming that the observed improvements are not due to chance and underscoring the effectiveness of the fusion approach even at relatively low levels of ACC^{movement} . As ACC^{movement} increases, the disparity between the naïve and fusion forecasts increases significantly.

Figure 3 illustrates the fusion results that are closest to the mean performance at each level of ACC^{movement} . When ACC^{movement} slightly exceeds 0.50, such as in the second plot where $ACC^{\text{movement}} = 0.55$, the fusion forecast shows only minor deviations from the naïve forecast and still exhibits a noticeable “shift” from the previous actual values. As ACC^{movement} increases, this “shift” progressively diminishes and vanishes when $ACC^{\text{movement}} = 1$.

Figure 4 illustrates the performance of the fusion forecasts across various accuracy levels using different fixed weights. As shown in the first four plots, under a smaller value of c , such as 0.01 or 0.1, the fusion forecast generally outperforms

Table 1: Predictions with different accuracies and optimal c values.

| Prediction | MSE | | MAE | |
|-----------------------|-------------------|---------|-------------------|---------|
| | Range | p value | Range | p value |
| Naïve | 1.044 | - | 0.821 | - |
| Acc = 0.50, $c = 0$ | 1.044 | - | 0.821 | - |
| Acc = 0.55, $c = 0.1$ | 1.037 ± 0.011 | 0.0000 | 0.816 ± 0.005 | 0.0000 |
| Acc = 0.60, $c = 0.2$ | 1.017 ± 0.026 | 0.0000 | 0.802 ± 0.012 | 0.0000 |
| Acc = 0.65, $c = 0.3$ | 0.982 ± 0.039 | 0.0000 | 0.775 ± 0.018 | 0.0000 |
| Acc = 0.70, $c = 0.4$ | 0.939 ± 0.044 | 0.0000 | 0.745 ± 0.019 | 0.0000 |
| Acc = 0.75, $c = 0.5$ | 0.885 ± 0.052 | 0.0000 | 0.712 ± 0.022 | 0.0000 |
| Acc = 0.80, $c = 0.6$ | 0.794 ± 0.051 | 0.0000 | 0.664 ± 0.022 | 0.0000 |
| Acc = 0.85, $c = 0.7$ | 0.716 ± 0.056 | 0.0000 | 0.623 ± 0.022 | 0.0000 |
| Acc = 0.90, $c = 0.8$ | 0.618 ± 0.055 | 0.0000 | 0.578 ± 0.023 | 0.0000 |
| Acc = 0.95, $c = 0.9$ | 0.493 ± 0.042 | 0.0000 | 0.526 ± 0.018 | 0.0000 |
| Acc = 1, $c = 1$ | 0.371 | - | 0.482 | - |

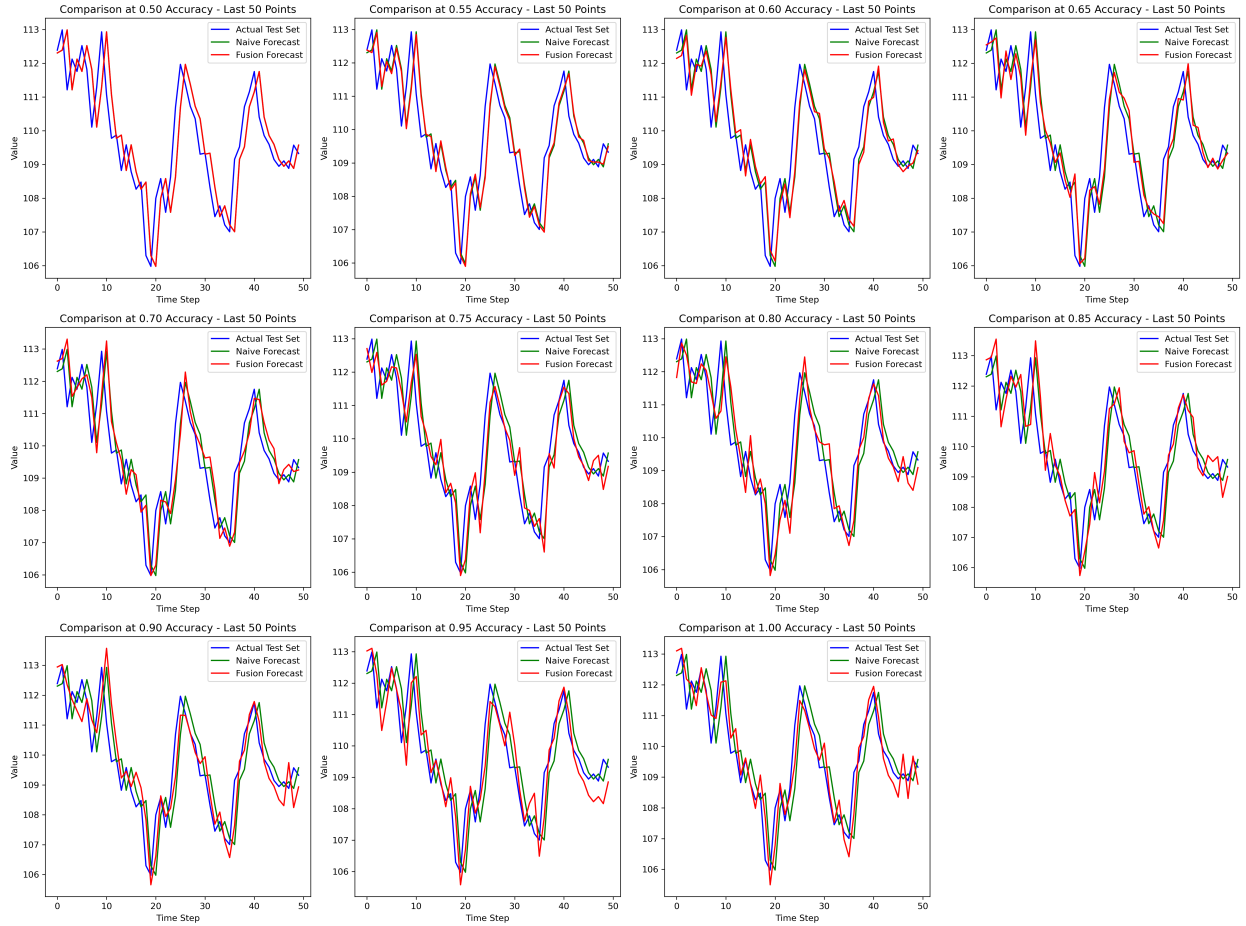


Figure 3: Fusion forecasts across different movement prediction accuracies.

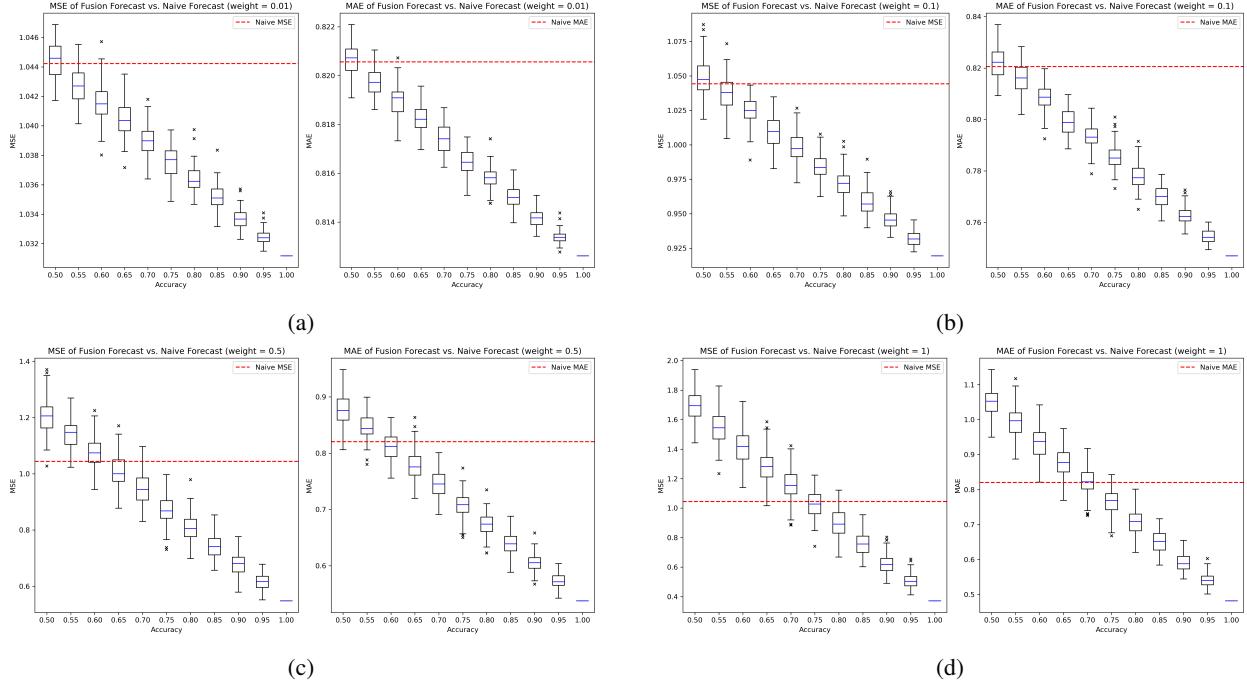


Figure 4: Forecasting performance of fusion across different accuracy levels using fixed weights: a) $c = 0.01$; b) $c = 0.1$; c) $c = 0.5$; d) $c = 1$.

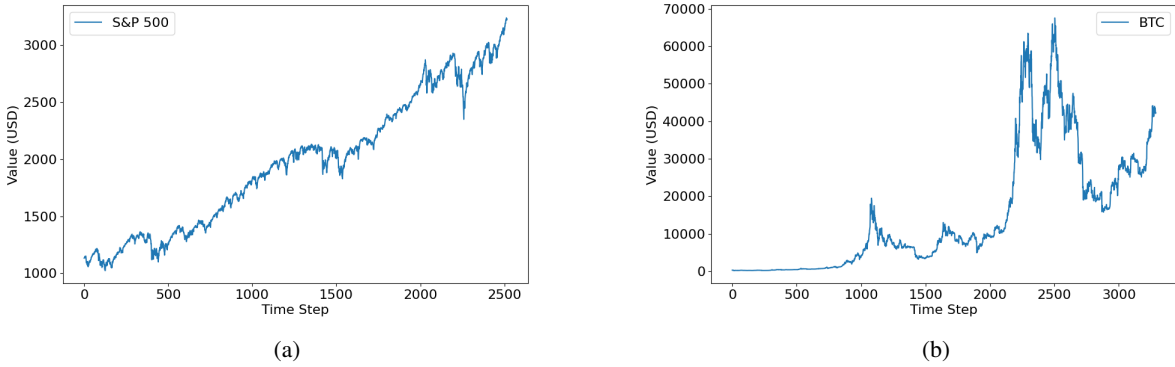


Figure 5: Real-world random walks: a) S&P 500; b) BTC.

the naïve forecast, albeit at the expense of potential gains from higher c . Conversely, setting a larger c could lead to inferior performance to the naïve forecast if the actual ACC^{movement} is poor. As long as ACC^{movement} is better than 0.5, setting a small value to weight c can ensure that the fusion result has an improvement compared to the naïve forecast, regardless of the actual value of ACC^{movement} .

4.2 Experiment 2: Real-world Data

Two real-world random walk series, the S&P 500 and BTC series, were selected for testing the performance of the proposed method based on real data and real movement predictions. Both sets of time series data were retrieved from Yahoo Finance. The raw data of the S&P 500 series cover historical daily closing prices from January 1, 2010, to December 31, 2019. For BTC, the data spanned from January 1, 2015, to December 31, 2023. The two univariate random walk series are shown in Figure 5 and are briefly described in Table 2.

Table 3 presents the augmented Dickey–Fuller (ADF) test results for the two real-world time series. The ADF test can identify the presence of a unit root, assessing whether the S&P 500 and BTC price series exhibit random walk

Table 2: Statistics of two real-world random walks.

| Time series | Count | Mean | Standard Deviation | Minimum | Median | Maximum |
|-------------|-------|----------|--------------------|---------|---------|----------|
| S&P 500 | 2516 | 1962.61 | 588.79 | 1022.58 | 1986.48 | 3240.02 |
| BTC | 3287 | 15041.63 | 16239.73 | 178.10 | 8659.49 | 67566.83 |

Table 3: Augmented Dickey–Fuller test of two real-world random walks.

| Time series | ADF Statistic | p value | Critical Values | | |
|-------------|---------------|----------|-----------------|--------|--------|
| | | | 1% | 5% | 10% |
| S&P 500 | 0.416927 | 0.982117 | -3.433 | -2.863 | -2.567 |
| BTC | -1.329129 | 0.615743 | -3.432 | -2.862 | -2.567 |

characteristics. For the S&P 500, the ADF statistic was 0.416927, with a p value of 0.982117. Given the critical values at the 1% (-3.433), 5% (-2.863), and 10% (-2.567) significance levels, the ADF statistic does not surpass these thresholds, and the high p value further supports the nonrejection of the null hypothesis. This suggests that the S&P 500 series likely follows a random walk, in which future values primarily reflect random fluctuations from previous values. Similarly, the BTC price series showed an ADF statistic of -1.449327 and a p value of 0.558413, with critical values not exceeded. This result indicates that the BTC price series is nonstationary and may also follow a random walk.

Each of the two datasets was split into distinct sets for model evaluation and hyperparameter tuning. Specifically, the last 200 data points of each series were allocated as the test set, whereas the second-to-last 200 points served as the validation set for tuning the model’s hyperparameters through a random search of 32 trials [Bergstra and Bengio \(2012\)](#). Data normalization was performed using a min–max scaling approach to standardize the inputs to a range between zero and one.

Although the accuracy of financial time series movement forecasts can range between 0.55 and 0.8, this study opted to not employ complex models that integrate external data sources, which are resource intensive. Instead, this study utilized the nu-support vector machine (nu-SVM), a reliable binary classification model with the proportion of support vectors tuned through a parameter nu [Bishop and Nasrabadi \(2006\)](#). This choice allows us to focus on testing the robustness of the fusion method under real movement prediction with moderate accuracy rather than pursuing higher accuracy through more sophisticated models, as previous simulations have adequately demonstrated the performance of the fusion method across different accuracy levels. In addition, the details regarding the feature extraction process, which leverages a range of technical indicators and market statistics as model inputs, are outlined in Table A.1 in the Appendix. The nu-SVM prediction accuracy on the validation set was used as an estimation of ACC^{movement} for setting the value of c based on (11).

Four baseline models, namely, ARIMA, linear regression, MLP, and LSTM, were selected for model performance comparison. For the LSTM model, input sequences were prepared using a sliding window of 50 time steps, which was designed to capture essential contextual information without imposing excessive computational burdens. Each input sequence, accompanied by its subsequent data point as the ground-truth label, was progressively generated by sliding the window one step forward through the series. For the linear regression and MLP models, the input features were the same as those employed for movement prediction. For the training of the MLP and LSTM models, the hyperparameters were iteratively optimized over 200 training epochs, and the Adam optimizer was used alongside the MSE as the cost function. The hyperparameter settings of the nu-SVM and the baseline models are presented in Table 4.

Figure 6 and Figure 7 present the forecasts of different methods for the S&P 500 and BTC series, respectively. Because the movement prediction accuracy on the validation set is approximately 0.55 for both time series, the weight c for the fusion method is set to 0.1. Consistent with the theoretical analysis presented in Section 3.2, this small weight c leads to a small discrepancy between the naïve and fusion forecasts. Complex models such as MLP and LSTM differ significantly from fusion, naïve, and ARIMA forecasts because they presuppose a mapping from historical sequences to future values, which should depend solely on the current value with a random increment. The assumed patterns and dependencies in the data obtained by these models may not exist in true random walks.

Table 5 summarizes the model performances in terms of the MSE and MAE values. The fusion method demonstrated the best overall performance among the models tested, achieving lower MSE and MAE values than did the naïve, ARIMA, and linear regression methods for both prediction tasks. Specifically, the fusion method yielded an MSE of 490.91 and an MAE of 16.19 for the S&P 500 prediction and an MSE of 449611.83 with an MAE of 431.94 for the BTC prediction, suggesting that the proposed method has a robust ability to make forecasts with reduced errors

Table 4: Hyperparameter settings.

| Model | Hyperparameter | Range |
|---------------------------|-----------------------------|------------|
| nu-SVM | nu | 0.1 to 0.9 |
| | kernel | “rbf” |
| Linear Regression (Ridge) | alpha | 0 to 10 |
| MLP | number of neurons per layer | 1 to 100 |
| | number of hidden layers | 2 |
| LSTM | number of hidden units | 50 to 300 |
| | learning rate | 0.0005 |

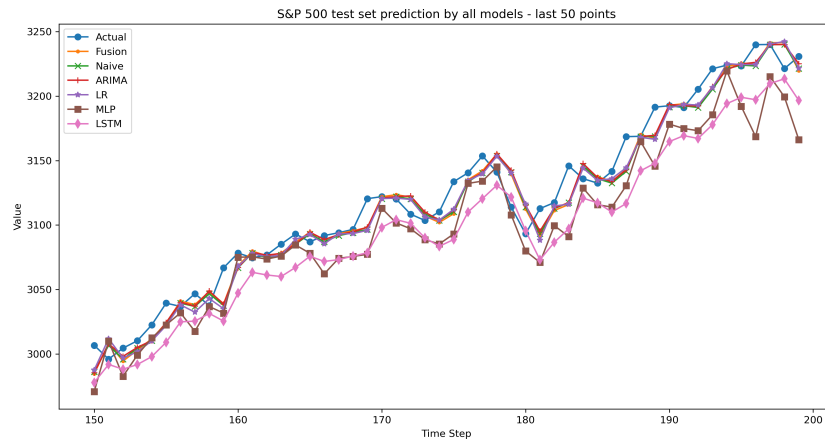


Figure 6: The S&P 500 forecast results of different methods.

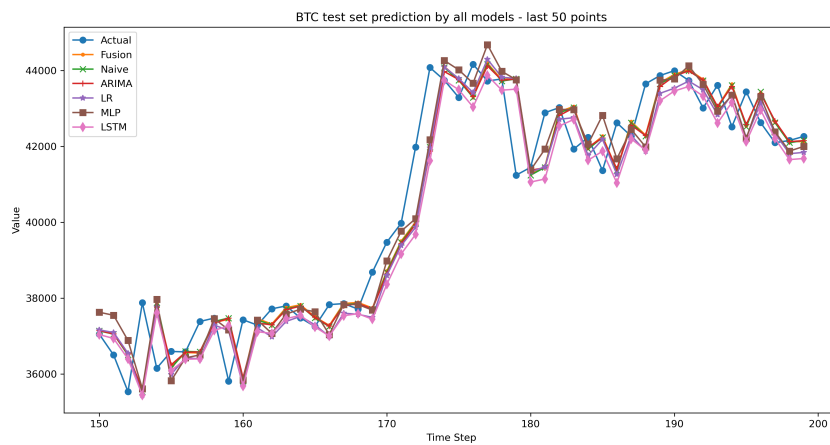


Figure 7: The BTC forecast results of different methods.

Table 5: Performance evaluation of different methods.

| Models | S&P 500 | | BTC | |
|-------------------|------------|-----------|---------------|------------|
| | MSE | MAE | MSE | MAE |
| Fusion | 490.912977 | 16.187902 | 449611.828348 | 431.940881 |
| Naïve | 499.378612 | 16.277100 | 456875.143422 | 433.766817 |
| ARIMA | 499.739638 | 16.338302 | 456466.453451 | 431.050006 |
| Linear Regression | 497.368764 | 16.236584 | 486329.417207 | 463.574310 |
| MLP | 775.427551 | 21.615049 | 486248.250000 | 496.776367 |
| LSTM | 690.336853 | 21.148510 | 503120.968750 | 457.213593 |

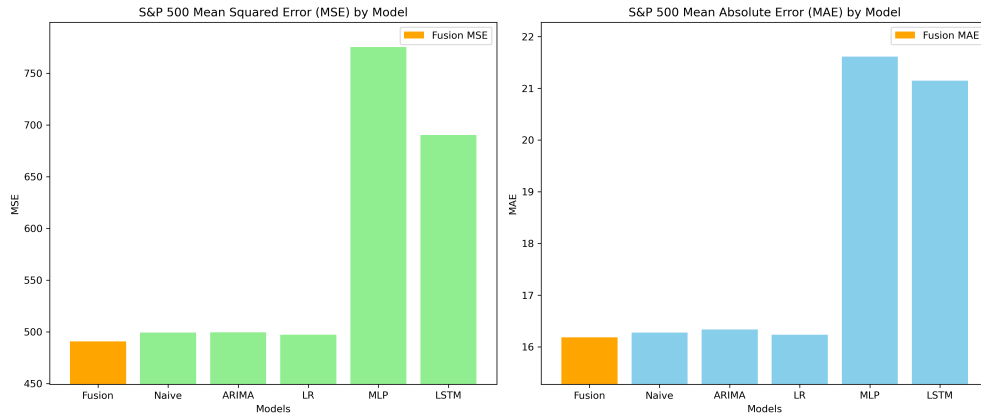


Figure 8: Comparison of the S&P 500 forecast errors of different methods.

compared to other models. In contrast, both the MLP and LSTM models underperformed compared with the more traditional approaches, showing particularly high forecasting errors for both prediction tasks.

Furthermore, Figure 8 and Figure 9 visualize the performance comparisons of different models applied to the two prediction tasks. The consistent performance of the fusion method on both prediction tasks highlights its robustness and effectiveness in forecasting random walk series compared with baseline models.

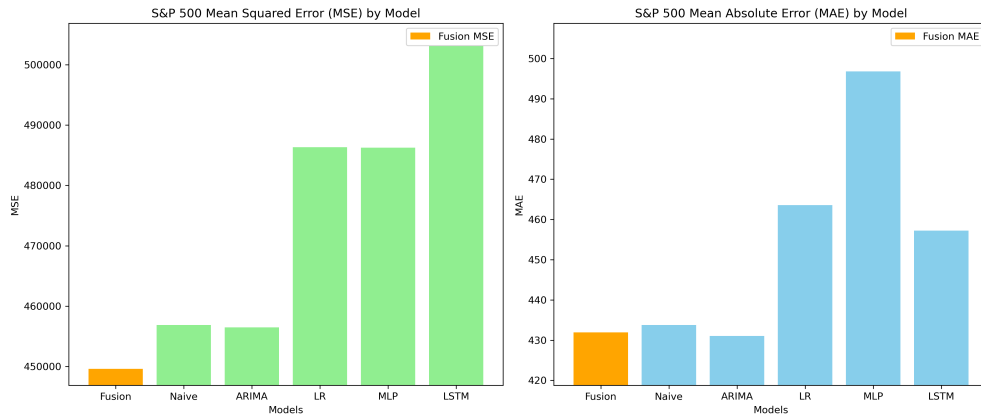


Figure 9: Comparison of the BTC forecast errors of different methods.

5 Discussion

This section discusses the implications of the findings based on theoretical analysis and experimental results and the potential limitations of this study. The empirical results show that when the ACC^{movement} is approximately 0.55, the proposed fusion method outperforms the naïve forecast, which is consistent with the theoretical expectation that a movement prediction accuracy above 0.5 is necessary. Interestingly, the movement prediction accuracy of financial time series can reach as high as 0.8 in specific scenarios [Bustos and Pomares-Quimbaya \(2020\)](#), indicating that high movement prediction for real-world random walks is possible and can potentially lead to fusion results better than the examples shown in this study. Nonetheless, in real forecasting scenarios, ACC^{movement} can only be estimated through model performance on the training or validation set, and such estimations can overestimate or underestimate the true ACC^{movement} . Whether ACC^{movement} on the test set can consistently meet the accuracy threshold for improvement remains a challenge.

From the simulations of the fusion results, it is observed that among the multiple trials of the fusion process at moderate accuracy levels, such as 0.55 and 0.60, some trials still underperformed compared to the naïve forecasts. However, the significant discrepancy between the median results of these trials and the naïve forecasts suggests that adopting an ensemble approach after each fusion process can achieve a more robust improvement over the naïve forecast.

Furthermore, the proposed fusion method can be viewed as a classification-to-regression conversion in the context of univariate time series forecasting. This is particularly useful when integrating diverse predictions is advantageous, but effectively combining predictions from models that produce different types of data, such as binary and continuous outputs, is challenging [Bishop and Nasrabadi \(2006\)](#); [Zhang et al. \(2022\)](#). The fusion method in this study effectively converts binary classifications into continuous values, enabling the integration of diverse data types. This conversion facilitates an efficient integration process, allowing for comprehensive use of available forecasts to improve decision-making in real forecasting scenarios.

Notably, the dataset used for experiments may not be large enough to meet the assumptions made in the theoretical analysis. In addition, while the definition of a random walk adopted in this study assumes i.i.d. increments for each time step, real-world data can be drifted random walks and are subject to measurement errors. All these factors could explain the discrepancies between the theoretical and empirical fusion results. Moreover, this study assumes the random increments to be the same for all future time steps, which may not always provide a reliable estimation owing to the fluctuating nature of real-world data.

6 Conclusion

This study introduced a novel fusion method specifically designed for point forecasting in univariate random walks. Key findings reveal that the fusion method can outperform naïve forecasts with moderate movement prediction accuracies, such as 0.55. This improvement is achieved without consuming large amounts of computational resources and significantly exceeds that of many traditional forecasting methods, which often fail to surpass naïve forecasts. The implications of these results are profound, suggesting that the fusion method offers a potent approach for enhancing the forecasting of random walk series by effectively utilizing movement predictions.

The theoretical analysis of this fusion method not only enriches the academic understanding of forecasting but also provides a robust framework for practical applications in areas where random walk forecasting is important. In addition, the demonstration of this approach in improving the point forecasts of financial time series paves the way for its application across a range of forecasting scenarios in different areas.

There are several avenues for further research that build upon the foundations laid by this study. First, although this research focuses on random walk forecasting, future work could expand the forecasting philosophy presented in this paper to encompass other types of time series data, potentially broadening its applicability. Second, given the dependency of the proposed method on movement predictions, which are still challenging in various areas, there is a pressing need to develop more advanced movement prediction techniques for random walk series. Such advancements, along with the fusion method proposed in this study, could contribute more to real random walk forecasting tasks.

Moreover, the current model utilizes a fixed increment for simplicity; however, adapting this increment based on the availability of new data may provide more dynamic and accurate forecasts. Investigating whether such adaptive increments can further refine the forecasting accuracy represents a promising direction for future research. This adaptive approach could lead to more nuanced and responsive forecasting models, potentially transforming predictive analytics in various areas.

Appendix

Code availability: <https://github.com/Zhang-Cheng-76200/Random-Walk-Prediction.git>

Table A.1: Feature extraction based on historical trading data.

| Feature Name | Description or Formula Used |
|------------------|--|
| return | $\text{Return} = \frac{\text{Close}_t - \text{Close}_{t-1}}{\text{Close}_{t-1}}$ |
| SMA_5 | $\text{SMA}_5 = \frac{1}{5} \sum_{i=t-4}^t \text{Close}_i$ |
| SMA_15 | $\text{SMA}_{15} = \frac{1}{15} \sum_{i=t-14}^t \text{Close}_i$ |
| SMA_ratio | $\text{SMA ratio} = \frac{\text{SMA}_{15}}{\text{SMA}_5}$ |
| SMA5_Volume | $\text{SMA5 Volume} = \frac{1}{5} \sum_{i=t-4}^t \text{Volume}_i$ |
| SMA15_Volume | $\text{SMA15 Volume} = \frac{1}{15} \sum_{i=t-14}^t \text{Volume}_i$ |
| SMA_Volume_Ratio | $\text{SMA Volume Ratio} = \frac{\text{SMA5 Volume}}{\text{SMA15 Volume}}$ |
| prev_close | Prev Close = Close_{t-1} |
| TR | $\text{TR} = \max(\text{High}_t - \text{Low}_t)$ |
| Lowest_5D | $\text{Lowest 5D} = \min(\text{Low}_{t-4}, \dots, \text{Low}_t)$ |
| High_5D | $\text{High 5D} = \max(\text{High}_{t-4}, \dots, \text{High}_t)$ |
| Lowest_15D | $\text{Lowest 15D} = \min(\text{Low}_{t-14}, \dots, \text{Low}_t)$ |
| High_15D | $\text{High 15D} = \max(\text{High}_{t-14}, \dots, \text{High}_t)$ |
| Stochastic_5 | $\text{Stochastic 5} = \frac{\text{Close}_t - \text{Lowest 5D}}{\text{High 5D} - \text{Lowest 5D}} \times 100$ |
| Stochastic_15 | $\text{Stochastic 15} = \frac{\text{Close}_t - \text{Lowest 15D}}{\text{High 15D} - \text{Lowest 15D}} \times 100$ |
| Stochastic_Ratio | $\text{Stochastic Ratio} = \frac{\text{Stochastic \%D5}}{\text{Stochastic \%D15}}$ |
| Diff | Diff = $\text{Close}_t - \text{Close}_{t-1}$ |
| Up | Up = $\max(\text{Diff}, 0)$ |
| Down | Down = $\max(-\text{Diff}, 0)$ |
| avg_5up | avg 5up = Up rolling mean over 5 days |
| avg_5down | avg 5down = Down rolling mean over 5 days |
| avg_15up | avg 15up = Up rolling mean over 15 days |
| avg_15down | avg 15down = Down rolling mean over 15 days |
| RS_5 | $\text{RS 5} = \frac{\text{avg 5up}}{\text{avg 5down}}$ |
| RS_15 | $\text{RS 15} = \frac{\text{avg 15up}}{\text{avg 15down}}$ |
| RSI_5 | $\text{RSI 5} = 100 - \left(\frac{100}{1 + \text{RS 5}} \right)$ |
| RSI_15 | $\text{RSI 15} = 100 - \left(\frac{100}{1 + \text{RS 15}} \right)$ |
| RSI_ratio | $\text{RSI Ratio} = \frac{\text{RSI 5}}{\text{RSI 15}}$ |
| 5Ewm | 5Ewm = Close ewm span=5, adjust=False mean() |
| 15Ewm | 15Ewm = Close ewm span=15, adjust=False mean() |
| MACD | MACD = 15Ewm - 5Ewm |
| 15MA | 15MA = Close rolling mean over 15 days |
| SD | SD = Close rolling std deviation over 15 days |
| upperband | upperband = 15MA + 2 × SD |
| lowerband | lowerband = 15MA - 2 × SD |
| RC | RC = Close percentage change over 15 days |

Acknowledgments

This study did not receive any specific grants from funding agencies in the public, commercial, or not-for-profit sectors.

References

Adhikari and Agrawal(2014). A combination of artificial neural network and random walk models for financial time series forecasting. *Neural Computing and Applications*, 24(6):1441–1449. doi: 10.1007/s00521-013-1386-y.

- Bengio(2011). Deep learning of representations for unsupervised and transfer learning.
- Bergstra and Bengio(2012). Random search for hyper-parameter optimization. *Journal of machine learning research*, 13(2).
- Bishop and Nasrabadi(2006). *Pattern recognition and machine learning*, volume 4. Springer.
- Bustos and Pomares-Quimbaya(2020). Stock market movement forecast: A systematic review. *Expert Systems with Applications*, 156:15. doi: 10.1016/j.eswa.2020.113464
- Chen et al.(2016). Financial time-series data analysis using deep convolutional neural networks. In *2016 7th International conference on cloud computing and big data (CCBD)*, pages 87–92. IEEE.
- Cheng et al.(2015). Time series forecasting for nonlinear and non-stationary processes: a review and comparative study. *IIE Transactions*, 47(10):1053–1071. doi: 10.1080/0740817X.2014.999180.
- Das et al.(2018). A compton suppressed detector multiplicity trigger based digital daq for gamma-ray spectroscopy. *Nuclear Instruments and Methods in Physics Research Section A: Accelerators, Spectrometers, Detectors and Associated Equipment*, 893:138–145. doi: 10.1016/j.nima.2018.03.035.
- De Gooijer(2017). *Elements of nonlinear time series analysis and forecasting*, volume 37. Springer.
- Deboeck(1994). *Trading on the edge: neural, genetic, and fuzzy systems for chaotic financial markets*, volume 39. John Wiley & Sons.
- Durairaj and Mohan(2019). A review of two decades of deep learning hybrids for financial time series prediction. *International Journal on Emerging Technologies*, 10(3):324–331.
- Ellwanger and Snudden(2023). Forecasts of the real price of oil revisited: Do they beat the random walk? *Journal of Banking & Finance*, 154:106962. doi: 10.1016/j.jbankfin.2023.106962.
- Fama(1995). Random walks in stock market prices. *Financial analysts journal*, 51(1):75–80.
- Frigg and Hartmann(2018). Models in science. *Stanford encyclopedia of philosophy (Summer 2018 Ed.)*. URL <https://plato.stanford.edu/archives/sum2018/entries/models-science>.
- Goodfellow et al.(2016). *Deep learning*. MIT press (Chapter 15).
- Gudelek et al.(2017). A deep learning based stock trading model with 2-d cnn trend detection. In *2017 IEEE Symposium Series on Computational Intelligence (SSCI)*, pages 1–8. doi: 10.1109/SSCI.2017.8285188.
- Hewamalage et al.(2023). Forecast evaluation for data scientists: common pitfalls and best practices. *Data Mining and Knowledge Discovery*, 37(2):788–832. doi: 10.1007/s10618-022-00894-5.
- Hochreiter and Schmidhuber(1997). Long short-term memory. *Neural computation*, 9(8):1735–1780.
- Jiang(2021). Applications of deep learning in stock market prediction: Recent progress. *Expert Systems with Applications*, 184. doi: 10.1016/j.eswa.2021.115537.
- Lara-Benítez et al.(2021). An experimental review on deep learning architectures for time series forecasting. *International Journal of Neural Systems*, 31(03):2130001. doi: 10.1142/S0129065721300011
- Malibari et al.(2021). Predicting stock closing prices in emerging markets with transformer neural networks: The saudi stock exchange case. *International Journal of Advanced Computer Science and Applications*, 12(12):876–886. doi: 10.14569/IJACSA.2021.01212106
- Matsubara et al.(2018). Stock price prediction by deep neural generative model of news articles. *IEICE Transactions on Information and Systems*, E101.D(4):901–908. doi: 10.1587/transinf.2016IIP0016.
- Moosa and Burns(2014). The unbeatable random walk in exchange rate forecasting: Reality or myth? *Journal of Macroeconomics*, 40:69–81. doi: 10.1016/j.jmacro.2014.03.003.
- Nelson et al.(2017). Stock market’s price movement prediction with lstm neural networks. In *2017 International Joint Conference on Neural Networks (IJCNN)*, pages 1419–1426. doi: 10.1109/IJCNN.2017.7966019.
- Nosratabadi et al.(2020). Data science in economics: Comprehensive review of advanced machine learning and deep learning methods. *Mathematics*, 8(10):25. doi: 10.3390/math8101799.
- Pearson(1905). The problem of the random walk. *Nature*, 72(1865):294–294. doi: 10.1038/072294b0.
- Raza(2017). Prediction of stock market performance by using machine learning techniques. In *2017 International conference on innovations in electrical engineering and computational technologies (ICIEECT)*, pages 1–1. IEEE.
- Rouf et al.(2021). Stock market prediction using machine learning techniques: A decade survey on methodologies, recent developments, and future directions. *Electronics*, 10(21):2717. doi: 10.3390/electronics10212717.

- Sezer and Ozbayoglu(2018). Algorithmic financial trading with deep convolutional neural networks: Time series to image conversion approach. *Applied Soft Computing*, 70:525–538. doi: 10.1016/j.asoc.2018.04.024.
- Sezer et al.(2017). A deep neural-network based stock trading system based on evolutionary optimized technical analysis parameters. *Procedia Computer Science*, 114:473–480. doi: 10.1016/j.procs.2017.09.031.
- Sezer et al.(2020). Financial time series forecasting with deep learning: A systematic literature review: 2005–2019. *Applied soft computing*, 90:106181. doi: 10.1016/j.asoc.2020.106181
- Shi et al.(2017). An end-to-end trainable neural network for image-based sequence recognition and its application to scene text recognition. *IEEE Transactions on Pattern Analysis and Machine Intelligence*, 39(11):2298–2304. doi: 10.1109/TPAMI.2016.2646371.
- Taylor(2008). *Modelling financial time series*. world scientific.
- Thakkar and Chaudhari(2021). Fusion in stock market prediction: A decade survey on the necessity, recent developments, and potential future directions. *Information Fusion*, 65:95–107. doi: 10.1016/j.inffus.2020.08.019.
- Troiano et al.(2018). Replicating a trading strategy by means of lstm for financial industry applications. *IEEE Transactions on Industrial Informatics*, 14(7):3226–3234. doi: 10.1109/TII.2018.2811377.
- Tsantekidis et al.(2020). Using deep learning for price prediction by exploiting stationary limit order book features. *Applied Soft Computing*, 93:106401. doi: 10.1016/j.asoc.2020.106401.
- Wang et al.(2018). Combining the wisdom of crowds and technical analysis for financial market prediction using deep random subspace ensembles. *Neurocomputing*, 299:51–61. doi: 10.1016/j.neucom.2018.02.095.
- Wergen et al.(2012). Record statistics for multiple random walks. *Physical Review E*, 86(1):011119. doi: 10.1103/PhysRevE.86.011119.
- Wu et al.(2022). Deterministic and uncertainty crude oil price forecasting based on outlier detection and modified multi-objective optimization algorithm. *Resources Policy*, 77:102780. doi: 10.1016/j.resourpol.2022.102780.
- Wu et al.(2021) Autoformer: Decomposition transformers with auto-correlation for long-term series forecasting. *Advances in neural information processing systems*, 34:22419–22430.
- Yang et al.(2017). Stock market index prediction using deep neural network ensemble. In *2017 36th chinese control conference (ccc)*, pages 3882–3887. IEEE.
- Yoshihara et al.(2014). Predicting stock market trends by recurrent deep neural networks. In Duc-Nghia Pham and Seong-Bae Park, editors, *PRICAI 2014: Trends in Artificial Intelligence*, pages 759–769. Springer International Publishing.
- Zhang et al.(2022). Decision Fusion for Stock Market Prediction: A Systematic Review. *IEEE Access*, 10:81364-81379. doi: 10.1109/ACCESS.2022.3195942.
- Zhang et al.(2023). Deep learning models for price forecasting of financial time series: A review of recent advancements: 2020–2022. *WIREs Data Mining and Knowledge Discovery*, 14(1):e1519. doi: 10.1002/widm.1519.
- Zhang et al.(2015). A novel hybrid method for crude oil price forecasting. *Energy Economics*, 49:649–659. doi: 10.1016/j.eneco.2015.02.018.
- Zhang(1999). Toward a theory of marginally efficient markets. *Physica A: Statistical Mechanics and its Applications*, 269(1):30–44.